

Bloch-Siegert Shift in a Hybrid Quantum Register: Quantification and Compensation

Jingfu Zhang¹, Sagnik Saha^{1,2} and Dieter Suter¹

¹ Fakultät Physik, Technische Universität Dortmund,
D-44221 Dortmund, Germany

² current address : Indian Institute of Science Education and Research Kolkata,
Mohanpur, India-741246

(Dated: June 8, 2018)

Quantum registers that combine the attractive properties of different types of qubits are useful for many different applications. They also pose a number of challenges, often associated with the large differences in coupling strengths between the different types of qubits. One example is the non-resonant effect that alternating electromagnetic fields have on the transitions of qubits that are not targeted by the specific gate operation. The example being studied here is known as Bloch-Siegert shift. Unless these shifts are accounted for and, if possible, compensated, they can completely destroy the information contained in the quantum register. Here we study this effect quantitatively in the important example of the nitrogen vacancy (NV) center in diamond and demonstrate how it can be eliminated.

PACS numbers: 03.67.Pp, 03.67.Lx

I. INTRODUCTION

Storage and processing of information in quantum mechanical systems, known as quantum information processing [1, 2], has an enormous potential for many applications where classical systems can not provide sufficient computational power. The realization of this potential relies, amongst others, on the capability to selectively apply gate operations to specific quantum bits (qubits), without perturbing the other qubits present in the system. In most systems that are currently being studied for this type of applications, the selection of the qubits is performed in frequency space: An alternating electric or magnetic field whose frequency is tuned to the transition frequency of the targeted qubit drives the target qubit in a way that can be well described by a rotation on the Bloch sphere. This type of resonant excitation works well for many different systems, such as electronic and nuclear spins, trapped atomic ions or neutral atoms, but also engineered systems like superconducting circuits [3].

The required selectivity of this frequency-domain addressing scheme is typically assumed to work well if the Rabi frequency of the driving field is small compared to the frequency difference between the qubits. As an example, if two qubits have transition frequencies Ω_A and Ω_B , the Rabi frequency ω_1 should fulfill the condition $|\omega_1| \ll |\Omega_A - \Omega_B|$ - a condition that can often be fulfilled.

The situation becomes more complicated in systems where the coupling strength between the qubits and the resonant field differs strongly between the different qubits. A particularly important type of such hybrid quantum registers are systems that consist of electronic and nuclear spins. The coupling strength between a spin and a magnetic field is quantified by the gyromagnetic ratio γ : $\omega_1 = \gamma B_1$, where B_1 is the amplitude of the AC magnetic field. If an alternating magnetic field is

used to drive the nuclear spin, the nuclear spin Rabi frequency is $\omega_{1n} = \gamma_n B_1$. The same field interacts also with the electron spin, and the corresponding Rabi frequency is $\omega_{1e} = |\gamma_e| B_1$, where $\gamma_e = -28$ GHz/T is the electronic gyromagnetic ratio, which is some three orders of magnitude larger than γ_n . In most cases, the condition $|\omega_{1e}| \ll |\Omega_e - \Omega_n| \approx |\Omega_e|$ is still well fulfilled and accordingly the resonant excitation of the electron spin is negligibly small. However, since the nuclear spin responds only slowly to the driving field, the gate operation is also several orders of magnitude longer than the electron spin operations. For such long pulse durations, also non-resonant effects can become relevant, in particular the Bloch-Siegert (BS) shift [4–6]: This effect can be described by an effective Hamiltonian for the transition where it is observed:

$$\frac{1}{2\pi} \mathcal{H}_{BS} = \omega_{BS} \frac{\sigma_z}{2}, \quad (1)$$

where σ_z denotes the z -component of the Pauli matrix. The frequency shift

$$\omega_{BS} = \frac{\omega_1^2}{2\omega_0} \quad (2)$$

is given by the square of the Rabi frequency ω_1 , divided by twice the transition frequency ω_0 . It can be calculated by the Floquet formalism [5], with a dressed atom model [7] or a unitary approach [8]. Here ω_0 denotes the transition frequency of the electron spin. The effect has been observed, e.g. in pulsed ENDOR [9], circuit quantum electrodynamics systems [10–12], and Rydberg atoms [13].

Clearly, this effect becomes large when strong pulses are used, such as in the ultra-strong coupling regime [14–22]. In the case of high-fidelity quantum control, the effects are smaller but no less relevant, since they may significantly degrade the fidelity of the operations [23, 24]. Here, we investigate the BS effects that RF pulses

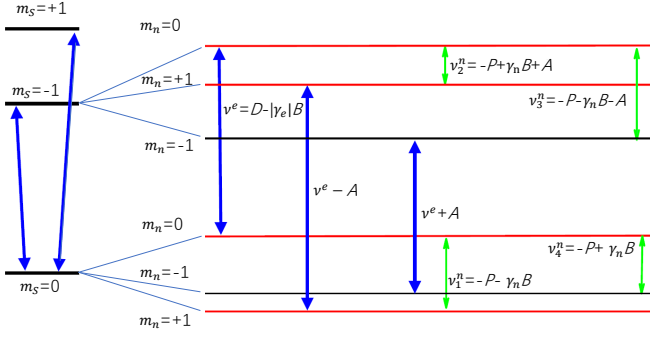


FIG. 1: (color online). Energy diagram of the NV center coupled with ^{14}N spin. The four basis states marked by red horizontal lines form a 2-qubit system. The vertical arrows indicate the allowed ESR and NMR transitions. The transition frequencies are indicated next to the arrows.

have on the electron spin of a nitrogen vacancy (NV) center in diamond.

II. SYSTEM AND EXPERIMENTAL PROTOCOL

We demonstrate the issue for the example of a system consisting of the electron and ^{14}N nuclear spins in a single NV center, subjected to a magnetic field B oriented along its symmetry axis. The Hamiltonian for this system can be written as [25, 26]

$$\frac{1}{2\pi} \mathcal{H} = DS_z^2 - \gamma_e BS_z + PI_z^2 - \gamma_n BI_z + AS_z I_z. \quad (3)$$

Here S_z and I_z are the z -components of the spin-1 operators for electronic and nuclear spins, respectively. The zero-field splitting is $D = 2.87$ GHz, the nuclear quadrupolar splitting $P = -4.95$ MHz, the hyperfine coupling $A = -2.16$ MHz [25, 27, 28] and the nuclear gyromagnetic ratio $\gamma_n = 3.1$ MHz/T. In the experiments, the static field strength is about 15 mT, which results in a separation of the two electron spin resonance (ESR) transitions by about 840 MHz.

Figure 1 shows the corresponding energy level scheme, focusing on the case where we excite the $m_s = 0 \leftrightarrow -1$ transitions of the electron spin. The ESR transition frequency was $\nu_1^e = 2438.739$ MHz, the NMR transition frequencies were $\nu_1^n = 4.990$, $\nu_2^n = 2.828$, $\nu_3^n = 7.066$, and $\nu_4^n = 4.898$ MHz, and the nuclear spin Rabi frequencies were 10.7, 6.0, 6.3, and 10.4 kHz at an RF power of $p_0 \approx 80$ mW. As a minimal system for the purpose of this demonstration, we focus on the four levels marked by thick red lines, which form a 2-qubit system.

Figure 2 shows the spectra of the ESR transitions between the states with $m_s = 0$ and -1 , obtained in a Ramsey-type free-induction decay (FID) experiment, using resonant microwave (MW) pulses with Rabi frequencies of about 10 MHz for excitation and detection.

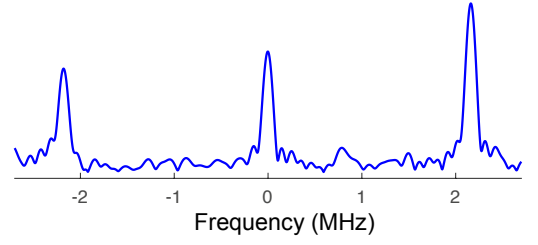


FIG. 2: (color online). Spectrum of the ESR transitions between the states with $m_s = 0$ and -1 , obtained as Fourier-transform of the time-domain signals. The origin of the frequency axes is set to $D - |\gamma_e|B$, measured as 2438.739 MHz.

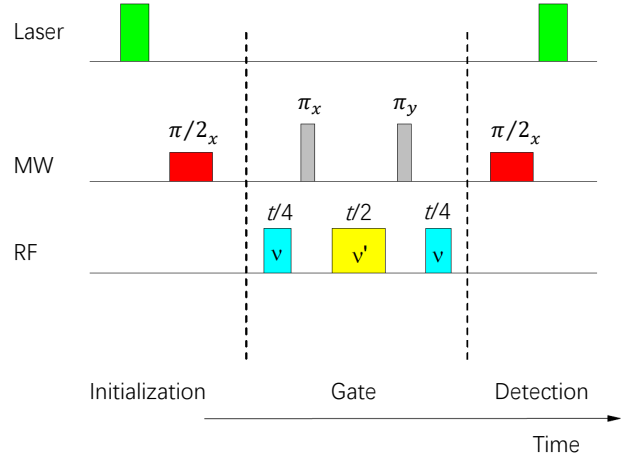


FIG. 3: (color online). Pulse sequence. The laser pulses ($\lambda = 532$ nm) are used for initialization and detection of the electron spin. The MW pulses are resonant with the transition $|0\rangle_e |0\rangle_n \leftrightarrow |-1\rangle_e |0\rangle_n$. In the initialization and detection steps, they are either transition-selective or hard pulses with Rabi frequency of about 0.30 MHz or 12 MHz, respectively. The flip angles are $\pi/2$, with the phase indicated by the index. During the gate, the MW pulses are hard pulses with Rabi frequency about 12 MHz. The frequencies of the RF pulses are indicated in the rectangles.

Figure 3 shows the pulse sequence used to demonstrate the effect and its compensation. During the initialization, we use a laser pulse to bring the electron spin to the $m_s = 0$ state, and then a MW pulse with a $\pi/2$ flip angle to generate coherence between the $m_s = 0$ and -1 states. This coherence allows us to observe the effect of the BS shift, which is generated by the radio frequency (RF) pulses during the period marked as “gate” in figure 3. These RF pulses are required to drive gate operations on the ^{14}N nuclear spin. The color (blue, yellow) of the pulses and the frequency labels (ν , ν') of the pulses indicate, with which transition they are resonant. During the gaps in the RF pulses, we apply dynamical decoupling (DD) pulses to the electron spin, to refocus unwanted dephasing of the electron spin coherence. During

the detection period, the MW pulse transforms the coherence to spin population and the laser pulse reads out the population of the $m_S = 0$ state $P_{|0\rangle}$.

III. MEASUREMENT OF THE FREQUENCY SHIFT

The applied RF field is oriented at an arbitrary direction with respect to the coordinate system of the NV center and has therefore components parallel as well as perpendicular to the NV-axis. The parallel component, which corresponds to the z -component in the conventional choice of coordinate system, leads to oscillations with the frequency of the RF field [29]. Here, we focus on the transverse components, which generate the BS-shift. To quantitate the observed effect and verify the interpretation as a BS shift, we measured the dependence of the shift on the the RF-amplitude. For this purpose, we applied RF pulses only before the first and after the second DD pulse. In the initialization and detection steps, we used transition selective MW pulses with the carrier frequency set to the transition $|0\rangle_e|0\rangle_n \leftrightarrow |-1\rangle_e|0\rangle_n$. The $\pi/2$ MW pulse in the initialization step generates a superposition of the electron spin

$$|s_0\rangle = (|0\rangle - i|1\rangle)/\sqrt{2}. \quad (4)$$

The z -rotation by the Hamiltonian (1) in the gate step

$$U_{BS}(t) = e^{-i2\pi\omega_{BS}t\sigma_z/4}, \quad (5)$$

turns $|s_0\rangle$ into

$$|s(t)\rangle = (|0\rangle e^{-i2\pi\omega_{BS}t/4} - i|1\rangle e^{i2\pi\omega_{BS}t/4})/\sqrt{2}. \quad (6)$$

During the detection step, the second $\pi/2$ MW pulse transforms $|s(t)\rangle$ to the final state

$$|s_f(t)\rangle = |0\rangle \cos(2\pi\omega_{BS}\frac{t}{4}) + |1\rangle \sin(2\pi\omega_{BS}\frac{t}{4}), \quad (7)$$

where the population $P_{|0\rangle}$ of $|0\rangle$ encodes the BS shift. Figure 4 shows the experimental results. for RF powers from zero to 80 mW. In the absence of an RF field, the electron spin coherence decays exponentially and we could fit the experimental data with the function

$$P_{|0\rangle} = a_1 + b_1 e^{-(t/T_2)^k}, \quad (8)$$

and obtained $T_2 = 1.3$ ms and $k = 1.2$.

To test the effect of the RF field, we first set the frequency far from the nuclear spin transitions and applied RF power during the first and third period of the gate (blue pulses in Fig. 3). The top three traces of Figure 4 show the resulting signals from the electron spin, measured with an RF frequency of $\nu = 6$ MHz and RF powers of $p_0 = 80$ mW, $p_0/2$, and $p_0/4$. The data can be fitted as

$$P_{|0\rangle} = a_2 + b_2 \cos(2\pi\frac{\omega_{BS}}{2}t)e^{-(t/T_2)}. \quad (9)$$

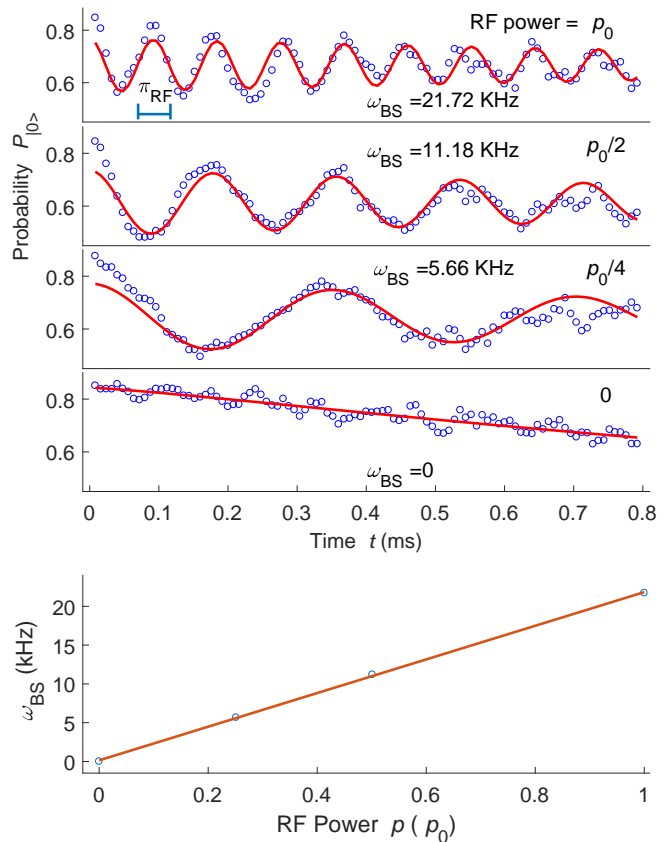


FIG. 4: (color online). Experimental results for the dependence of the BS shift on the amplitude B_1 of the RF pulses. The RF frequency was 6 MHz and the RF power was p_0 , $p_0/2$, and $p_0/4$ and 0. The horizontal scale bar in the panel for RF power p_0 indicates the duration of the π pulse for the ^{14}N spin when the RF frequency is resonant with the transition at 4.990 MHz. The experimental data are shown as empty circles. The fit to the data, shown as the solid curves, gave the frequencies $\omega_{BS} = 21.72$, 11.18 and 5.66 kHz. The bottom trace shows the dependence of ω_{BS} on the RF power, with the measured data as empty circles, and a linear fit to the data.

The resulting fit parameters are $\omega_{BS} = 21.72$, 11.18 and 5.66 kHz for decreasing power. The bottom trace of figure 4 shows the dependence of the measured frequency on the RF power. According to Eq. (2), the dependence should be linear (quadratic in B_1), which is well borne out by the experimental data.

In the second set of experiments, we fixed the power of the RF pulses to p_0 and varied the frequency from 6.5 MHz to 7 and 7.5 MHz. By fitting the data using function (9), with different constant a_2 and b_2 , we obtained the oscillation frequency as $\omega_{BS} = 21.34$, 20.88 and 20.90 kHz, as illustrated in Figure 5. Within the experimental uncertainty, the oscillation frequency does not depend on the RF frequency, as shown in the bottom part of Figure 5. This result is also consistent with the prediction of Eq. (2).

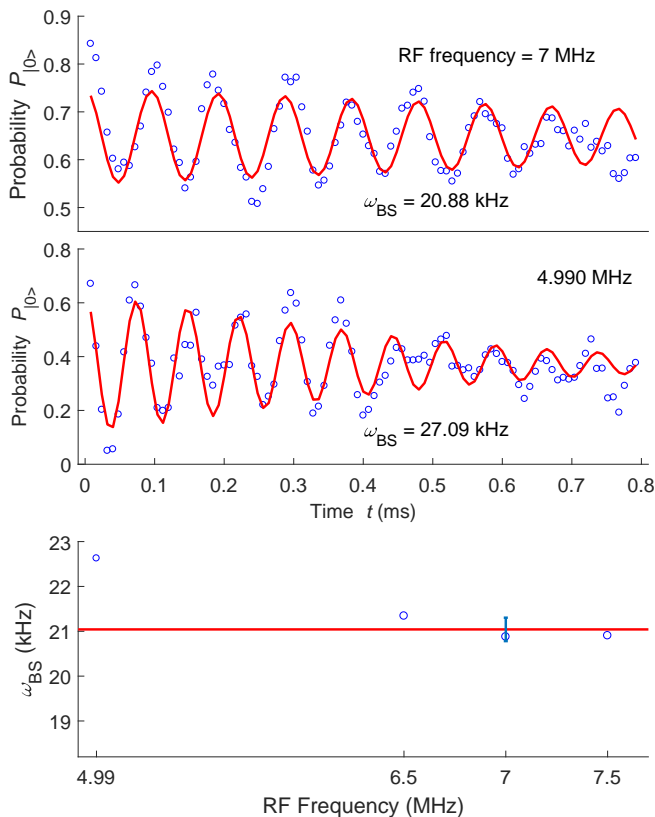


FIG. 5: (color online). Measurement of the BS shift as a function on the frequency of the RF pulses, obtained with the first and third RF pulses at power p_0 . The experimental data are shown as circles and the RF frequencies are indicated in the panels. By fitting the data, shown as the solid curves, we obtained the BS shift indicated in the panel. In the bottom figure, we show the measured BS shift by the empty circles for RF frequencies 6.5, 7, and 7.5 MHz. The solid line shows the average, and the error bar shows the standard deviation. Since the RF power was not constant as a function of frequency, we normalized the shift observed at 4.99 MHz to the same RF power as the others.

For the case that the RF pulses are resonant with the NMR transitions, they affect the nuclear as well as the electronic spin. In order to eliminate this effect and observe only the BS shift, we use hard pulses in the initialization and detection steps. In this case, we can neglect the small polarization of the nuclear spin, shown as the small difference in the peak amplitudes of Figure 2. We applied RF pulses with frequency $\nu = \nu_1^n = 4.990$ MHz. The results are shown in Figure 5. By fitting the data using the function in Eq. (9), we obtained $\omega_{BS} = 27.09$ kHz. The deviation from the results in the off-resonant case can be mainly attributed to the difference of the powers. We therefore normalized the measured ω_{BS} to the applied power; the result is shown in the bottom part of Figure 5. It is close to the average value measured in the off-resonant case.

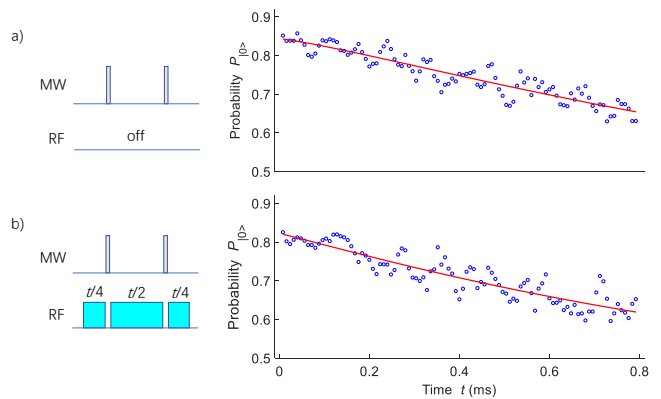


FIG. 6: (color online). Cancellation of the BS shift by DD pulses, indicated by the grey narrow rectangles. The experimental data are indicated by the empty circles, and the fits with Eq. (8) by solid curves. (a) Without RF: no shift, decay of the coherence with $T_2 = 1.3$ ms and $k = 1.2$. (b) All the RF pulses in the sequence are switched on and have the same frequency (6 MHz) and power p_0 . The experimental data can be fitted with $T_2 = 1.2$ ms and $k = 1.1$.

IV. COMPENSATION

Since the BS shift corresponds to a quasi-static shift of the resonance frequency, it can be eliminated by applying refocusing pulses, provided it is constant for the whole period. For this demonstration, we use a very simple DD sequence consisting of one π_x and one π_y pulse, as shown in Fig. 3. The total phase generated by the RF pulses, which are applied only between the DD pulses, is then $\phi_{BS} = \phi_1 - \phi_2 + \phi_3$, where the three terms denote the phase acquired before the first, between the two and after the second DD pulse. If the RF power is constant and the relative pulse durations are 1:2:1, the total phase vanishes, $\phi_{BS} = 0$.

In Figure 6, we illustrate the experimental results in the case of off-resonant RF pulses with power p_0 and frequency $\nu' = \nu = 6$ MHz, and compare it to the case without RF. In both cases, we observe no oscillations, indicating that the phases generated by the different pulses cancel each other completely. We can use function (8) to fit the non-oscillatory data, and obtained the fitted $T_2 = 1.2$ and 1.3 ms for data with and without RF pulses. The similarity between the results with and without RF pulses shows the good cancellation of the BS shift, consistent with the prediction in previous work [29].

V. DISCUSSION

Since the BS shift is sensitive to the RF power but independent of the RF frequency, it might be a valuable resource to measure or calibrate the RF power using the electron spin as a probe. One potential application could be for estimating the perpendicular component A_{\perp} of the hyperfine coupling from ^{14}N in the NV center system. In

principle, one can extract A_{\perp} from the measured Rabi frequencies of ^{14}N , using the different enhancement for different states of the ^{14}N [30]. However this strategy requires that the response of the electronics to a change of the RF frequency is known precisely. Although this response can be partially corrected by measuring the RF power, the deviation is still not small enough, shown as the data in the bottom plot in Figure 5.

In order to normalize the RF power for measuring Rabi frequencies of ^{14}N , we can set an offset, e.g., 0.5 MHz from the concerned NMR transition, noting that the RF power in such a range can be treated as a constant, shown as the experimental data in the bottom plot in Figure 5. Since the maximal Rabi frequencies are about 10 kHz in our experiment, the offset of 0.5 MHz is large enough to avoid the resonance effect from the NMR transition. Therefore we can normalize the RF power by measuring the BS effect using the protocol proposed in the current paper. Then we can extract A_{\perp} from the corrected Rabi frequencies.

VI. CONCLUSION

In conclusion, we have demonstrated that AC magnetic fields that are used to drive the nuclear spins in a hybrid

quantum register can have a large effect on the electronic spin although their frequency is very far from their resonance frequencies. The main effect is a phase shift, which can easily exceed 2π and therefore completely scramble the quantum information stored in the electron spin qubit, unless measures are taken to eliminate its effect. The purpose of this work was to quantitatively measure the effect and test schemes for compensation. We have analyzed the dependence of the BS shift on the power and frequency of the RF pulses and demonstrated that spin echoes can refocus the BS effect with excellent precision.

VII. ACKNOWLEDGEMENT

This work was supported by the DFG through grant 192/34-1. S. Saha thanks the support by DAAD-WISE 2017 for financing his travel and stay in Germany to carry out the research project. We also thank Dr. Swathi Hegde for useful discussions.

-
- [1] M. A. Nielsen and I. L. Chuang, *Quantum Computation and Quantum Information* (Cambridge University Press, Cambridge, 2000).
 - [2] J. Stolze and D. Suter, *Quantum Computing: A Short Course from Theory to Experiment* (Wiley-VCH, Berlin, 2nd edition, 2008).
 - [3] T. D. Ladd, F. Jelezko, R. Laamme, Y. Nakamura, C. Monroe, and J. L. O'Brien, *Nature* **464**, 45 (2010).
 - [4] F. Bloch and A. Siegert, *Phys. Rev.* **57**, 522 (1940).
 - [5] J. H. Shirley, *Phys. Rev.* **138**, B979 (1965).
 - [6] L. Emsley and G. Bodenhausen, *Chem. Phys. Lett.* **168**, 297 (1990).
 - [7] C. Cohen-Tannoudji, J. Dupont-Roc, and C. Fabre, *Journal of Physics B: Atomic and Molecular Physics* **6**, L214 (1973).
 - [8] Y. Yan, Z. Lv, and H. Zheng, *Phys. Rev. A* **91**, 053834 (2015).
 - [9] M. Mehring, P. Hofer, and A. Grupp, *Phys. Rev. A* **33**, 3523 (1986).
 - [10] P. Forn-Diaz, J. Lisenfeld, D. Marcos, J. J. Garcia-Ripoll, E. Solano, C. J. P. M. Harmans, and J. E. Mooij, *Phys. Rev. Lett.* **105**, 237001 (2010).
 - [11] A. Baust, E. Hoffmann, M. Haeberlein, M. J. Schwarz, P. Eder, J. Goetz, F. Wulschner, E. Xie, L. Zhong, F. Quijandria, et al., *Phys. Rev. B* **93**, 214501 (2016).
 - [12] I. Pietikainen, S. Danilin, K. S. Kumar, A. Vepsalainen, D. S. Golubev, J. Tuorila, and G. S. Paraoanu, *Phys. Rev. B* **96**, 020501 (2017).
 - [13] D. Fregenal, E. Horsdal-Pedersen, L. B. Madsen, M. Førre, J. P. Hansen, and V. N. Ostrovsky, *Phys. Rev. A* **69**, 031401 (2004).
 - [14] A. Moroz, *Annals of Physics* **340**, 252 (2014).
 - [15] G. Gunter, A. A. Anappara, J. Hees, A. Sell, G. Biasiol, L. Sorba, S. D. Liberato, C. Ciuti, A. Tredicucci, A. Leitenstorfer, et al., *Nature* **458**, 178 (2009).
 - [16] L. S. Bishop, J. M. Chow, J. Koch, A. A. Houck, M. H. Devoret, E. Thuneberg, S. M. Girvin, and R. J. Schoelkopf, *Nature Physics* **5**, 105 (2009).
 - [17] T. Niemczyk, F. Deppe, H. Huebl, E. P. Menzel, F. Hocke, M. J. Schwarz, J. J. Garcia-Ripoll, D. Zueco, T. Hummer, E. Solano, et al., *Nature Physics* **6**, 772 (2010).
 - [18] K. R. K. Rao and D. Suter, *Phys. Rev. A* **95**, 053804 (2017).
 - [19] P. Forn-Diaz, J. J. Garcia-Ripoll, B. Peropadre, J.-L. Orgiazzi, M. A. Yurtalan, R. Belyansky, C. M. Wilson, and A. Lupascu, *Nature Physics* **13**, 39 (2017).
 - [20] F. Yoshihara, T. Fuse, S. Ashhab, K. Kakuyanagi, S. Saito, and K. Semba, *Nature Physics* **13**, 44 (2017).
 - [21] J. Braumüller, M. Marthaler, A. Schneider, A. Stehli, H. Rotzinger, W. Martin, and A. V. Ustinov, *Nature Communications* **8**, 779 (2017).
 - [22] J. Tuorila, M. Silveri, M. Sillanpää, E. Thuneberg, Y. Makhlin, and P. Hakonen, *Phys. Rev. Lett.* **105**, 257003 (2010).
 - [23] M. Steffen, L. M. K. Vandersypen, and I. L. Chuang, *Journal of Magnetic Resonance* **146**, 369 (2000).
 - [24] C. A. Ryan, C. Negrevergne, M. Laforest, E. Knill, and R. Laflamme, *Phys. Rev. A* **78**, 012328 (2008).
 - [25] C. S. Shin, M. C. Butler, H.-J. Wang, C. E. Avalos, S. J. Seltzer, R.-B. Liu, A. Pines, and V. S. Bajaj, *Phys. Rev. B* **89**, 205202 (2014).
 - [26] D. Suter and F. Jelezko, *Progress in Nuclear Magnetic*

- Resonance Spectroscopy **98-99**, 50 (2017)
- [27] X.-F. He, N. B. Manson, and P. T. H. Fisk, Phys. Rev. B **47**, 8816 (1993).
- [28] B. Yavkin, G. Mamin, and S. Orlinskii, J. Magn. Reson. **262**, 15 (2016).
- [29] M. Hirose and P. Cappellaro, Nature **532**, 77 (2016).
- [30] M. Chen, M. Hirose, and P. Cappellaro, Phys. Rev. B **92**, 020101 (2015)